IEEE Access
Multidisciplinary | Rapid Review | Open Access Journal

Received 3 April 2023, accepted 17 April 2023, date of publication 21 April 2023, date of current version 3 May 2023.

Digital Object Identifier 10.1109/ACCESS.2023.3269282

METHODS

Third-Harmonic Current Injection Control of Five-Phase Permanent-Magnet Synchronous Motor Based on Third-Harmonic Current Reference Online Identification

JIANHUA LI[1], BOCHAO DU[1,2], TIANXU ZHAO[1], YUAN CHENG[1,2], AND SHUMEI CUI[1]
[1]Department of Electrical Engineering and Automation, Harbin Institute of Technology, Harbin 150000, China
[2]Chongqing Research Institute, Harbin Institute of Technology, Chongqing 401135, China

Corresponding author: Bochao Du (dubochao@hit.edu.cn)

This work was supported in part by the National Key Research and Development Program of China under Grant 2019YFE0123500, and in part by the Fundamental Research Funds for the Central Universities under Grant FRFCU9803501121.

ABSTRACT The ratio of torque to copper loss can be increased by injecting third-harmonic current into five-phase permanent-magnetic synchronous motor (PMSM). Accurate flux linkage information is indispensable in the process of calculating third-harmonic current reference corresponding to the maximum torque/copper loss ratio. In harsh working environments, the flux linkage will deviate from the initial measured value, resulting in the deviation between the third-harmonic current and the maximum torque/copper working point. Therefore, a third-harmonic current injection control strategy of five-phase PMSM based on third-harmonic current reference online identification is proposed in this paper. The key of this strategy is to transform the steady-state voltage equations into an equation containing only voltages and currents. The transformed equation has a characteristic that it is equal to 0 when the motor operates at the maximum torque/copper loss ratio working point. Meanwhile, an observer is designed to estimate the third-harmonic current reference by using the characteristic. Finally, the observer is applied in third-harmonic current injection control of five-phase PMSM. Compared with previous methods, the proposed strategy is simple, no need of flux linkage information and not affected by the change of flux linkage. The experimental results demonstrate the robustness of the proposed strategy.

INDEX TERMS Five-phase permanent-magnetic synchronous motor, third-harmonic current injection, online identification.

I. INTRODUCTION

Multiphase motors are widely concerned because of their distinctive advantages, such as high reliability and low torque ripple [1], [2], [3]. Due to the above advantages, multiphase motors have broad applications in electric vehicles, aerospace, and ship propulsion. As a typical motor of multiphase motors, five-phase permanent-magnet synchronous motor (PMSM) combines the characteristics of multiphase motor and PMSM, and shows considerable advantages in efficiency, power density, dynamic performance, and fault-tolerance [4], [5]. Especially, five-phase PMSM is reported to be enhanced torque production using third-harmonic injection [6], [7]. With the rapid development of industrial technology, the motor requires higher torque density. The methods of improving motor torque density by using third-harmonic injection have caused tremendous attention.

Employing the optimal third-harmonic magnet shaping to obtain maximum fundamental flux within the flux limitation is a common method to improve the torque of PMSM [8], [9], [10], [11]. The peak of air-gap flux density is reduced by injecting the third-harmonic component to improve the utilization rate of permanent magnets. For three-phase PMSMs with balanced Y-connected windings, which

The associate editor coordinating the review of this manuscript and approving it for publication was Feifei Bu.

the third-harmonic current is naturally suppressed, it is unnecessary to consider the influence of the third-harmonic injection on the operation of the motor. However, for five-phase PMSMs, the current caused by the third-harmonic injection not only increases copper loss but also affects the operation of the motor. Therefore, the third-harmonic current is necessary to be considered in motor design and control. One method is to suppress the third-harmonic current to reduce copper loss and improve performance. In [12], double space vector control and multi-dimensional modulation method are combined to achieve the suppression of the third-harmonic current by the authors. However, it does not make full use of the torque output capacity of the motor. Another more competitive method is to inject the third-harmonic current to maximize the torque output. Third-harmonic current is used to couple with the third-harmonic spatial magnetomotive force (MMF) to yield additional average torque components. In [13], a five-phase PMSM, which has trapezoidal back electromotive force (EMF) and is supplied with the combined fundamental plus third-harmonic currents, has been verified to have better performance than the BLDC motor due to its controllability and compatibility with vector control technique by simulation and experiment. In [14], the authors found that, although the copper loss and iron loss increase due to additional third harmonics in the winding current and magnet shape, the average torque with optimal third harmonics injected in magnet shaping and current waveform can be improved by $>30\%$ while the torque ripple and remains similar to that of the one with sine shaping. In [15], it is found that torque improvement can be achieved by employing the unequal tooth structure in five-phase PMSM, and the torque improvement with the optimal third-harmonic current injection is only dependent on the ratio of the third-harmonic back EMF to the fundamental one. In addition to improving torque output through motor design, the matching control method to achieve third-harmonic injection is also of great research value.

Compared with model predictive control (MPC) and direct torque control (DTC), vector control has more advantages in harmonic injection due to its good performance and feature of easy implementation [2], [16], [17]. The double space vector control is the most common control method for third-harmonic current injection, which fundamental and third-harmonic components can be controlled effectively and independently to have the same initial phase and proper ratio of amplitude. In addition to the control structure, scholars pay more attention to optimize the reference of injected current. In [18], under the constraint of identical amplitude of phase current, the optimum ratio of the third-harmonic current is scanned by simulation. In [19], considering the voltage and current constraints, the optimal current references minimizing the dissipation and maximizing the torque is obtained. In [20], the authors studied the optimal ratio of injected current under three different optimization objectives, namely, the minimum copper loss, the minimum phase current amplitude, the minimum loss (copper loss and iron loss). To ensure the minimum torque loss ratio during the third harmonic current injection process, the working points with the minimum loss as the optimum objective is scanned through finite-element simulation. However, simulations add the limitation of application to the method, and the results are affected by manufacturing errors. Among the above optimization methods, the method with minimum copper loss as the optimization objective is widely used, due to its great advantages in practical applications, such as low thermal stress, high efficiency and easy application. Compared with other methods, simulation model is not needed in the process of calculating the third-harmonic current reference, only the flux linkage information is needed. The flux linkage information is usually obtained by measuring back EMF, which makes the realization of the method more complex, especially in the cases which motor parameters are not easy to measure. Moreover, in harsh working environments, the flux linkage will deviate from the initial measured value, resulting in the deviation between the third-harmonic current and the maximum torque/copper loss working point.

In this paper, a third-harmonic current injection control strategy of five-phase PMSM based on third-harmonic current reference online identification is proposed. Firstly, according to the torque equation, the expression of the third-harmonic current corresponding to the maximum torque copper loss ratio is derived. Secondly, the principle of the proposed online identification method is analyzed. On this basis, the third-harmonic current reference observer is designed and applied to the double space vector control. Finally, an experimental platform is built to verify the performance of the proposed strategy.

Compared with previous works, the contributions of this paper can be classified as follows: 1) It is found for the first time that, the steady-state voltage equations of the five-phase PMSM can be transformed into an equation containing only voltages and currents, and the characteristic of this equation is that it is equal to 0 when the motor operates at the maximum torque/copper loss ratio working point; and 2) a new third-harmonic current injection control strategy of five-phase PMSM for maximum torque copper loss ratio is proposed. The strategy obtains the third-harmonic current reference through online identification, which is simple, no need of flux linkage information and not affected by the change of flux linkage.

Meanwhile, the limitation of the proposed method can be summarized as: 1) the method is only applicable to five-phase PMSM with third harmonics in back EMF; and 2) the method fails at very low speed or standstill.

This paper is organized as follows. Section II analyzes the principle of the third-harmonic current injection with minimum copper loss as the optimization objective. Section III describes the proposed third-harmonic current injection control strategy of five-phase PMSM based on third-harmonic current reference online identification.

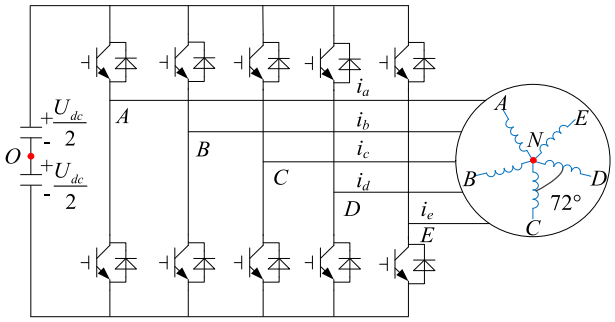

FIGURE 1. Configuration of five-phase PMSM drive.

In Section IV, experimental results are presented. The conclusion is drawn in Section V.

II. PRINCIPLE OF THE THIRD-HARMONIC CURRENT INJECTION BASED ON MINIMUM COPPER LOSS

A. MATHEMATICAL MODEL OF FIVE-PHASE PMSM

Fig.1 shows the configuration of the five-phase PMSM fed by the five-phase two-level voltage source inverter. The stator windings are star-connected, which are 72 electric degrees apart from each other spatially. The five-phase PMSM is a nonlinear high-order system, which makes the analysis and control difficult. By using the vector space decomposition (VSD), the phase-variable model can be transformed into the decoupled VSD model [2]. Without considering the zero-sequence components, the components of the phase-variable model can be decoupled into two two-dimensional orthogonal subspaces, namely fundamental and third-harmonic space.

The decoupled dynamic model of five-phase PMSM can be expressed as Equation (1) [21]. Where u_{d1} and u_{q1} are the fundamental space voltages; i_{d1} and i_{q1} are the fundamental space currents; u_{d3}, u_{q3} are the third-harmonic space voltages; i_{d3} and i_{q3} are the third-harmonic space currents; R_s is the stator resistance; L_{d1} and L_{q1} are inductances at fundamental space; L_{d3} and L_{q3} are inductances at third-harmonic space; p is the differential operator, ω is the rotor electrical speed, and ψ_{m1} is the fundamental permanent magnet flux linkage, ψ_{m3} is the third-harmonic permanent magnet flux linkage.

$$\begin{aligned}\begin{bmatrix} u_{d1} \\ u_{q1} \\ u_{d3} \\ u_{q3} \end{bmatrix} &= R_s \begin{bmatrix} i_{d1} \\ i_{q1} \\ i_{d3} \\ i_{q3} \end{bmatrix} + \begin{bmatrix} L_{d1} & 0 & 0 & 0 \\ 0 & L_{q1} & 0 & 0 \\ 0 & 0 & L_{d3} & 0 \\ 0 & 0 & 0 & L_{q3} \end{bmatrix} p \begin{bmatrix} i_{d1} \\ i_{q1} \\ i_{d3} \\ i_{q3} \end{bmatrix} \\ &+ \omega \begin{bmatrix} 0 & -L_{q1} & 0 & 0 \\ L_{d1} & 0 & 0 & 0 \\ 0 & 0 & 0 & -3L_{q3} \\ 0 & 0 & 3L_{d3} & 0 \end{bmatrix} \begin{bmatrix} i_{d1} \\ i_{q1} \\ i_{d3} \\ i_{q3} \end{bmatrix} \\ &+ \omega \begin{bmatrix} 0 \\ \psi_{m1} \\ 0 \\ 3\psi_{m3} \end{bmatrix} \end{aligned} \tag{1}$$

The electromagnetic torque T_e can be expressed as Equation (2).

$$\begin{aligned} T_e = \frac{5P_n}{2} \big[&\psi_{m1} i_{q1} + 3\psi_{m3} i_{q3} + \left(L_{d1} - L_{q1}\right) i_{d1} i_{q1} \\ &+ 3\left(L_{d3} - L_{q3}\right) i_{d3} i_{q3} \big] \end{aligned} \tag{2}$$

For surface-mounted five-phase PMSM, the air gap can be considered as uniform, so $L_{d1} = L_{q1}$, and $L_{d3} = L_{q3}$. Equation (2) can be rewritten and expressed as Equation (3).

$$T_e = \frac{5P_n}{2} \left[\psi_{m1} i_{q1} + 3\psi_{m3} i_{q3} \right] \tag{3}$$

It can be seen from Equation (3), in addition to fundamental component, third-harmonic component can also contribute to the torque output positively, which is the intrinsic argument for enhancing torque output.

B. THIRD-HARMONIC CURRENT INJECTION BASED ON MINIMUM COPPER LOSS

The RMS of phase current is restrained by the power capability of inverter and heat resistance of winding insulation. For the five-phase PMSM, the copper loss is proportional to the RMS of phase current. Therefore, the limitation of RMS of phase current is also considered as the limitation of copper loss. In order to achieve the maximum torque output within this limitation, the third-harmonic current is necessary to optimized. For surface-mounted five-phase PMSM, i_{d1} and i_{d3} are controlled to 0, because they have no contribution to torque output, but bring additional copper loss. The limitation can be expressed as Equation (4), where C is a positive constant.

$$i_{q1}^2 + i_{q3}^2 = C^2 \tag{4}$$

Define m as the $i_{q3}/\ i_{q1}$ ratio. i_{q1} and i_{q3} can be represent with m and C as Equation (5).

$$\begin{aligned} i_{q1} &= \frac{C}{\sqrt{1+m^2}} \\ i_{q3} &= \frac{Cm}{\sqrt{1+m^2}} \end{aligned} \tag{5}$$

Substituting Equation (5) into Equation (3). Equation (3) is rewritten and denoted as Equation (6).

$$\begin{aligned} T_e(m) &= \frac{5P_n}{2} \left[\psi_{m1} \frac{C}{\sqrt{1+m^2}} + 3\psi_{m3} \frac{Cm}{\sqrt{1+m^2}} \right] \\ &= \frac{5P_n C}{2} \frac{\left(\psi_{m1} + 3\psi_{m3} m\right)}{\sqrt{1+m^2}} \end{aligned} \tag{6}$$

All components in Equation (6) are not negative, and m is the only one variable. Therefore, extreme points can be obtained by differentiating the squares of $T_e(m)$. Equation (7) is obtained by differentiating the square of $T_e(m)$ with respect to m.

$$\frac{dT_e^2(m)}{dm} = \frac{25P_n^2 C^2}{2} \frac{\left(\psi_{m1} + 3\psi_{m3} m\right)\left(3\psi_{m3} - \psi_{m1} m\right)}{\left(1+m^2\right)^2} \tag{7}$$

According to Equation (7), when m is greater than $3\psi_{m3}/\psi_{m1}$, Equation (7) is less than 0. It means that the torque/copper loss ratio gradually decreases as m increases; When m is less than $3\psi_{m3}/\psi_{m1}$, Equation (7) is greater than 0. It means that the torque/copper loss ratio gradually decreases as m decreases; Therefore, when m is equal to $3\psi_{m3}/\psi_{m1}$, the maximum torque is achieved with the limitation of Equation (4).

III. PROPOSED STRATEGY BASED ON THIRD-HARMONIC CURRENT REFERENCE ONLINE IDENTIFICATION

A. PRINCIPLE OF THIRD-HARMONIC CURRENT REFERENCE ONLINE IDENTIFICATION

According to Equation (1), in the case that i_{d1} and i_{d3} are set to 0, the steady-state equations of five-phase PMSM can be expressed as Equation (8).

$$\begin{cases} u_{d1} = -\omega L_{q1} i_{q1} \\ u_{q1} = R_s i_{q1} + \omega \psi_{m1} \\ u_{d3} = -3\omega L_{q3} i_{q3} \\ u_{q3} = R_s i_{q3} + 3\omega \psi_{m3} \end{cases} \tag{8}$$

Multiplying both sides of the u_{q1} and u_{q3} voltage equations by i_{q3} and i_{q1} respectively. Equation (9) and Equation (10) can be obtained.

$$i_{q3} u_{q1} = i_{q3} \left(R_s i_{q1} + \omega \psi_{m1} \right) \tag{9}$$

$$i_{q1} u_{q3} = i_{q1} \left(R_s i_{q3} + 3\omega \psi_{m3} \right) \tag{10}$$

Equation (11) is obtained by subtracting Equation (9) from Equation (10).

$$i_{q1} u_{q3} - i_{q3} u_{q1} = \omega \left(3 i_{q1} \psi_{m3} - i_{q3} \psi_{m1} \right) \tag{11}$$

When m is equal to $3\psi_{m3}/\psi_{m1}$, the left side of Equation (11) is equal to 0; When m is greater than $3\psi_{m3}/\psi_{m1}$, the left side of Equation (11) is less than 0; When m is less than $3\psi_{m3}/\psi_{m1}$, the left side of Equation (11) is greater than 0. Therefore, the left side of Equation (11) can be used to observe the third-harmonic current reference corresponding to the maximum torque/copper loss ratio.

B. DESIGN OF OBSERVER

Under steady state, i_{q1} and i_{q3} are approximately equal to their reference i_{q1}^* and i_{q3}^* respectively. When m is approximately equal to $3\psi_{m3}/\psi_{m1}$, that is, the left side of Equation (11) is small enough. Equation (12) can be obtained.

$$i_{q1}^* \approx i_{q3}^* \frac{\psi_{m1}}{3\psi_{m3}} \tag{12}$$

Replacing $\hat{i}_{q3}^*$ with its estimated value $\hat{i}_{q3}^*$, the left side of Equation (11) can be simplified as Equation (13) by using Equation (12).

$$\begin{aligned} i_{q1} u_{q3} - i_{q3} u_{q1} &= i_{q1}^* u_{q3} - \hat{i}_{q3}^* u_{q1} = \omega \left(3 i_{q1}^* \psi_{m3} - \hat{i}_{q3}^* \psi_{m1} \right) \\ &= \omega \left(3 i_{q3}^* \frac{\psi_{m1}}{3\psi_{m3}} \psi_{m3} - \hat{i}_{q3}^* \psi_{m1} \right) \\ &= \omega \psi_{m1} \left(i_{q3}^* - \hat{i}_{q3}^* \right) = \omega \psi_{m1} \Delta i_{q3}^* \end{aligned} \tag{13}$$

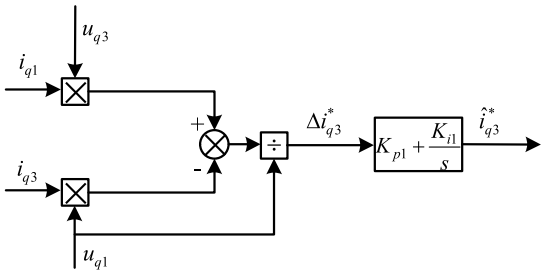

FIGURE 2. Third-harmonic current reference observer.

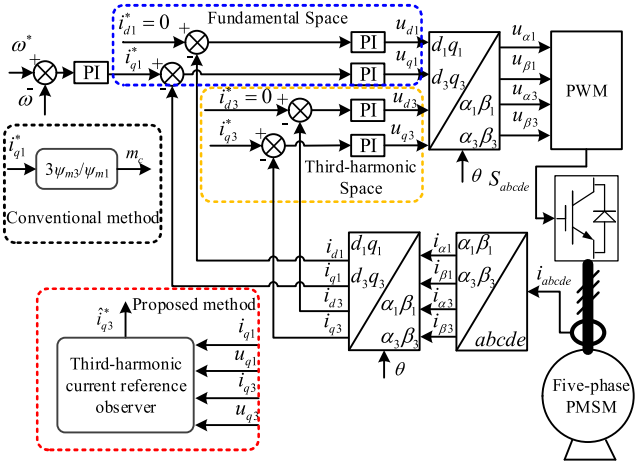

FIGURE 3. Double-space vector control based on third-harmonic current reference online identification.

According to Equation (13), if the left side of Equation (11) is used as the input of observer, the performance of the observer is affected by ω. It means that the performance of the observer changes with the changing of steady-state speed, which is unacceptable. To eliminate the influence, the input of the observer needs to be optimized. When the motor is running at middle or high speed, the stator resistance voltage drop is negligible, i.e, u_{q1} is approximately equal to $\omega\psi_{m1}$. Equation (14) is obtained by dividing the left side of Equation (11) by u_{q1}.

$$\frac{i_{q1} u_{q3} - i_{q3} u_{q1}}{u_{q1}} = \frac{\omega \psi_{m1} \left(i_{q3}^* - \hat{i}_{q3}^* \right)}{\omega \psi_{m1}} = \Delta i_{q3}^* \tag{14}$$

The left side of Equation (14) is used as the input of observer. According to Equation (14), i_{q3}^* corresponding to the maximum torque/copper loss ratio can be tracked with zero steady-state error by using a PI-type observer, due to the fact that it is constant in steady state. The structure of the PI-type observer is shown as Fig. 2. K_{p1} and K_{i1} are the proportional and integral gains respectively.

C. VECTOR CONTROL STRUCTURE OF THE PROPOSED STRATEGY

As shown in Fig. 3, the vector control is divided into the fundamental space and the third harmonic space. The torque output is realized by controlling the current at two spaces respectively. i_{d1}^*, i_{q1}^*, i_{d3}^* and i_{q3}^* are the references of i_{d1}, i_{q1}, i_{d3} and i_{q3} respectively. $\hat{i}_{q3}^*$ is the estimated value of i_{q3}^*.

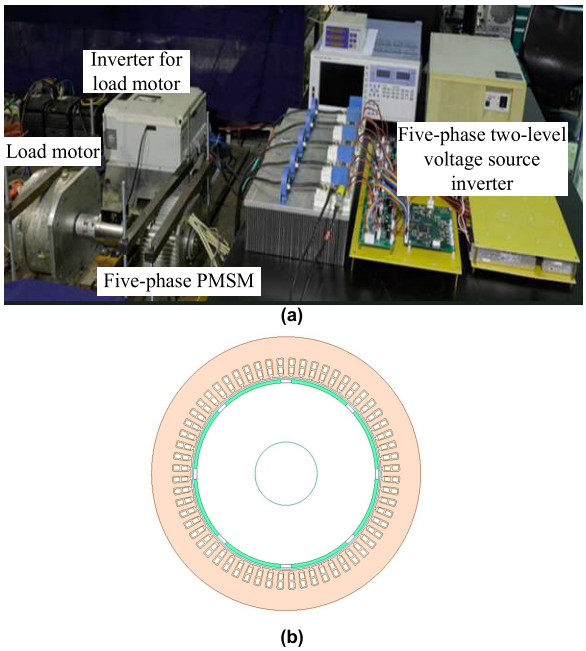

FIGURE 4. Configuration of experimental platform and motor: (a) ex-perimental platform and (b) sixty-slot/eight-pole inner rotor five-phase PMSM.

To avoid additional copper loss, i_{d1}^* and i_{d3}^* are set to 0. The output of speed loop is used as i_{q1}^*.

For the proposed method based on online identification, the output of third-harmonic current reference observer, namely $\hat{i}_{q3}^*$, is used as i_{q3}^*. The input of third-harmonic current reference observer is obtained from the current loops at both spaces. For the conventional method based on flux linkage calculation, m_c is used as i_{q3}^*. m_c is equal to the product of i_{q1}^* and $3\psi_{m3}/\psi_{m1}$.

Compared with the conventional method based on flux linkage calculation, the new method has several advantages, such as simple, no need of flux linkage information and not sensitive to the change of flux linkage. In addition, it is worth emphasizing that the proposed method fails at very low speed or standstill, due to the indirect use of flux linkage information.

IV. EXPERIMENTAL RESULTS

To verify the performance of the proposed third-harmonic current injection control strategy, an experimental platform of five-phase PMSM is implemented and a sixty-slot/eight-pole inner rotor five-phase PMSM is adopted, as shown in Fig. 4. The parameters of the five-phase PMSM are listed in Table 1. The five-phase PMSM is connected to a five-phase two-level voltage source inverter and a load motor is mechanically coupled with the five-phase PMSM to produce the load torque. The TMS320F28335 DSP is adopted to execute the control algorithm. The PWM switching frequency of the inverter is 10 kHz, and the dead time is 2.67 μs. A digital-to-analog converter AD5725 is employed to output the waveform. The parameters of the third-harmonic current reference observer are designed as $K_{p1} = 0.1$ and $K_{i1} = 2$.

TABLE 1. Parameters of Five-phase PMSM.

Parameters	Value
No. of pole pairs	4
Stator outer radius	68 mm
Stator inner radius	48 mm
Airgap length	3 mm
Axial length	46 mm
Rotor outer radius	45 mm
rated current	10 A
rated line voltage	100 V
rated torque	25 N
rated speed	800 rpm
fundamental rotor flux linkage, ψ_{m1}	0.1923 Wb
third-harmonic rotor flux linkage, ψ_{m3}	0.01299 Wb

When the windings are open circuit, the phase back EMF at 200 rpm is measured and shown in Fig. 5 (a). The FFT analysis of the measured phase back EMF in Fig. 5 (b) shows that the torque of the motor used in the experiment can be improved by third-harmonic injection.

The steady-state current waveforms at 800 rpm with rated load are shown in Fig. 6 (a), (b) and (c), corresponding to three different control strategies. When sinusoidal power supply strategy is adopted, i_{q1} and i_{q3} are 14.7 A and 0 A respectively; When flux linkage calculation strategy is adopted, i_{q1} and i_{q3} are 14.1 A and 2.8 A respectively; When the proposed online identification strategy is adopted, i_{q1} and i_{q3} are 13.9 A and 3.2 A respectively. It can be seen from the figures that the currents of three strategies are different under the condition of same speed and same torque. Moreover, the proposed strategy has good performance under steady-state condition.

Fig. 7 and Fig. 8 show the current working points and the $i_{q3}/\ i_{q1}$ ratios with torque changing at rated speed. Under the constraints of RMS, the optimal current working points are obtained by experimental testing. The experiment testing is aiming at scanning the amplitude of i_{q1} by adjusting the amplitude of i_{q3} by 0.1 A each time under the condition of constant torque. Among all the scanned working points, the working points with the smallest RMS are selected. The optimal current working points are used to illustrate the effectiveness of the proposed strategy. It can be seen from the figures that the working points of the two strategies are closed to the optimal working points which scanned by experimental testing. The maximum difference of the $i_{q3}/\ i_{q1}$ ratios between the two strategies and experimental testing is no more than 5%. Fig. 9 shows the RMS of currents with the same torque and speed. It can be seen from the figure that the RMS of current based on the proposed online identification strategy and flux linkage calculation is closed to the RMS of current based on experimental testing, which illustrates the performance of the proposed online identification strategy is similar to the flux linkage calculation strategy in terms of torque copper loss ratio. Compared with the strategy based on sinusoidal supply, both two strategies can effectively improve the torque/copper loss ratio.

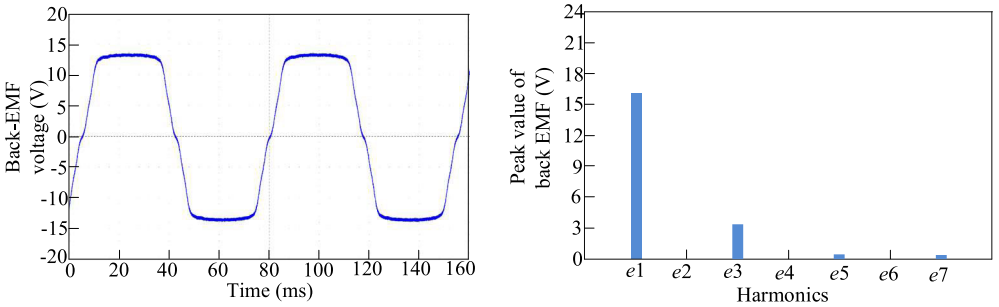

FIGURE 5. Back EMF of five-phase PMSM: (a) Phase back EMF waveform at 200 rpm and (b) FFT results of phase back EMF.

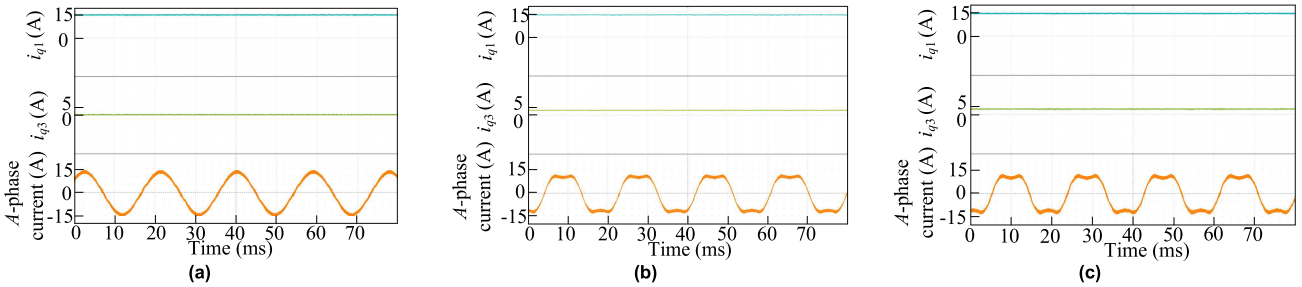

FIGURE 6. Current waveforms under three different control strategies: (a) strategy based on sinusoidal supply, (b) strategy based on flux linkage calculation and (c) proposed strategy based on online identification.

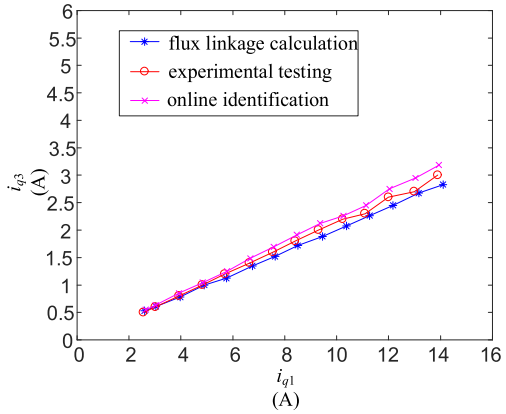

FIGURE 7. Comparison of the current working points.

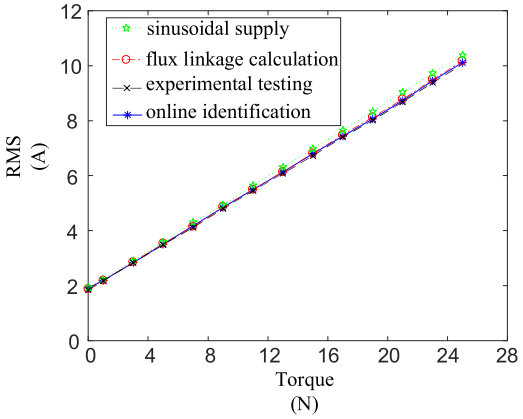

FIGURE 9. The RMS of currents.

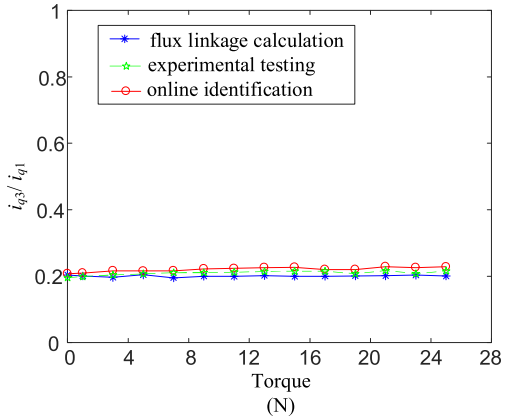

FIGURE 8. Comparison of the i_{q3}/i_{q1} ratios.

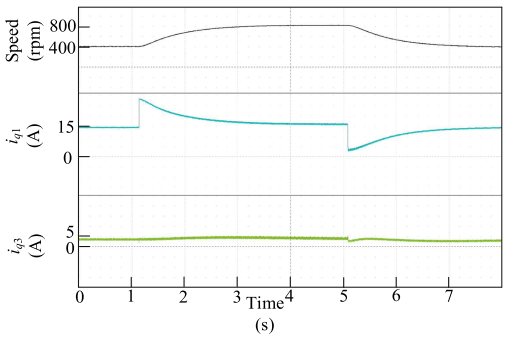

FIGURE 10. Online identification with speed changing.

Fig. 10 shows that the five-phase PMSM under the online identification strategy operates from 400 to 800 rpm, subsequently back to 400 rpm with rated load. Fig. 11 shows that the five-phase PMSM under the online identification strategy operates from 400 to 800 rpm, subsequently back to 400 rpm with rated load. The experimental results at 800 rpm

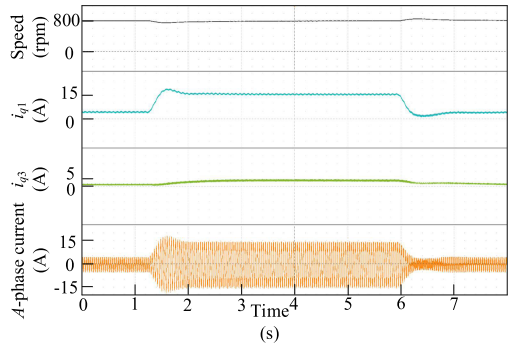

FIGURE 11. Online identification with torque changing.

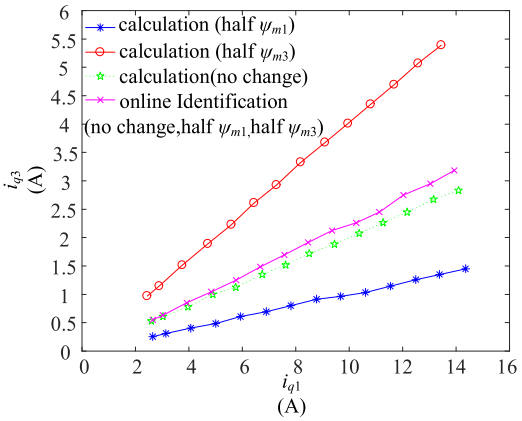

FIGURE 12. The current working points with flux linkage changing.

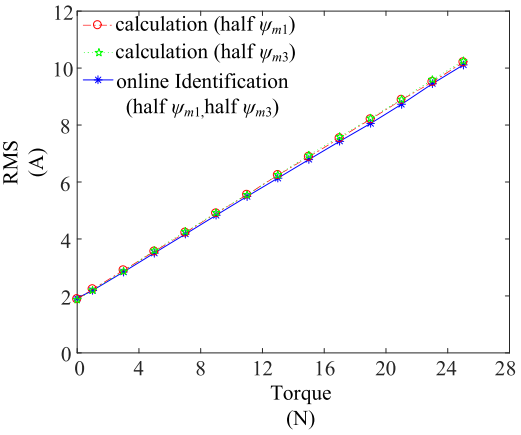

FIGURE 13. The RMS of currents with flux linkage changing.

for the proposed strategy based on online identification with a step disturbance are presented in Fig. 11. The step load disturbance is varied from 30% rate load to rate load and then back to 30% rate load. It can be seen from Fig. 10 and Fig. 11 that i_{q3} can follow i_{q1} quickly and maintain a certain proportion with it when the speed and torque of the motor change suddenly. The experimental result verifies that the proposed strategy has a good adaptability to the changes of speed and torque.

To verify the robustness of the proposed online identification strategy to the change of flux linkage, the strategy based on flux linkage calculation is compared with the proposed strategy in the case of flux linkage variations. The changes of flux linkage are realized by assuming the existing experimental motor is the motor with flux linkage changed. All experimental results are completed on the basis of this assumption. The current working points of both two strategies corresponding to no change, half ψ_{m1} and half ψ_{m3} are shown in Fig. 12. It can be found that when the flux linkage changes, the strategy based on flux linkage calculation deviates from the correct current working points, while the proposed online identification strategy tracks the correct current working points. Fig. 13 shows the RMS of current based on both two strategies with flux linkage changing. It can be found that the RMS of the current under the proposed online identification strategy is lower than the RMS of the current under flux linkage calculation strategy with the same load. It can be seen from Fig. 12 and Fig. 13 that the proposed online identification strategy is robust to the change of flux linkage.

V. CONCLUSION

In this paper, a third-harmonic current injection control strategy of five-phase PMSM based on third-harmonic current reference online identification is proposed to increase the ratio of torque to copper loss. It is found that when the ratio of injected current is equal to the ratio corresponding to the minimum copper loss, a new equation transformed from the steady-state equations has the characteristic of equal to 0. By using the characteristic, an observer is designed to obtain the third-harmonic current reference corresponding to maximum torque copper loss ratio. Meanwhile, the third-harmonic current injection control is realized by combining the observer with double space vector control. Compared with the conventional strategy based on flux linkage calculation, the proposed strategy is no need of flux linkage information and not sensitive to the change of flux linkage.

The feasibility of the proposed method was demonstrated via experiments. The results showed the good steady-state and dynamic performance. In conclusion, the proposed method is a promising candidate for five-phase PMSM third-harmonic injection, especially in the cases which flux linkages are not easy to measure.

REFERENCES

[1] E. Levi, F. Barrero, and M. J. Duran, "Multiphase machines and drives-revisited," *IEEE Trans. Ind. Electron.*, vol. 63, no. 1, pp. 429–432, Jan. 2016.

[2] F. Barrero and M. J. Duran, "Recent advances in the design, modeling, and control of multiphase machines—Part I," *IEEE Trans. Ind. Electron.*, vol. 63, no. 1, pp. 449–458, Jan. 2016.

[3] M. J. Duran and F. Barrero, "Recent advances in the design, modeling, and control of multiphase machines—Part II," *IEEE Trans. Ind. Electron.*, vol. 63, no. 1, pp. 459–468, Jan. 2016.

[4] W. Wang, Z. Song, Y. Liu, and C. Liu, "Decoupled modulation scheme for harmonic current suppression in five-phase PMSM," *IEEE Trans. Power Electron.*, vol. 37, no. 8, pp. 8795–8799, Aug. 2022.

[5] M. S. R. Saeed, W. Song, B. Yu, and X. Feng, "Generalized deadbeat solution for model predictive control of five-phase PMSM drives," *IEEE Trans. Power Electron.*, vol. 38, no. 4, pp. 5178–5191, Apr. 2023.

[6] J. Huang, Y. Sui, Z. Yin, S. Yang, and P. Zheng, "Five-phase hybrid single-/double-layer fractional slot-winding PMSM for torque improvement under third harmonic current injection condition," *IEEE Trans. Magn.*, vol. 58, no. 8, pp. 1–6, Aug. 2022.
[7] J. Huang, P. Zheng, Y. Sui, J. Zheng, Z. Yin, and L. Cheng, "Third harmonic current injection in different operating stages of five-phase PMSM with hybrid single/double layer fractional-slot concentrated winding," *IEEE Access*, vol. 9, pp. 15670–15685, 2021.
[8] Y. Li, J. Zou, and Y. Lu, "Optimum design of magnet shape in permanent-magnet synchronous motors," *IEEE Trans. Magn.*, vol. 39, no. 6, pp. 3523–3526, Nov. 2003.
[9] Z. Q. Zhu, K. Wang, and G. Ombach, "Optimal magnet shaping with third order harmonic for maximum torque in brushless AC machines," in *Proc. 6th IET Int. Conf. Power Electron., Mach. Drives (PEMD)*, Bristol, U.K., 2012, pp. 1–4.
[10] K. Wang, Z. Q. Zhu, and G. Ombach, "Torque enhancement of surface-mounted permanent magnet machine using third-order harmonic," *IEEE Trans. Magn.*, vol. 50, no. 3, pp. 104–113, Mar. 2014.
[11] W. Ullah, F. Khan, N. Ullah, and A. Majid, "Investigation of third harmonic utilization for torque performance improvement in novel H-type modular stator consequent pole machine," *Electr. Eng.*, vol. 2022, pp. 1–13, Feb. 2022.
[12] J. Li, B. Du, T. Zhao, Y. Cheng, and S. Cui, "Sensorless control of five-phase permanent-magnet synchronous motor based on third-harmonic space," *IEEE Trans. Ind. Electron.*, vol. 69, no. 8, pp. 7685–7695, Aug. 2022.
[13] L. Parsa and H. A. Toliyat, "Five-phase permanent-magnet motor drives," *IEEE Trans. Ind. Appl.*, vol. 41, no. 1, pp. 30–37, Jan./Feb. 2005.
[14] K. Wang, Z. Q. Zhu, and G. Ombach, "Torque improvement of five-phase surface-mounted permanent magnet machine using third-order harmonic," *IEEE Trans. Energy Convers.*, vol. 29, no. 3, pp. 735–747, Sep. 2014.
[15] Z. Y. Gu, K. Wang, Z. Q. Zhu, Z. Z. Wu, C. Liu, and R. W. Cao, "Torque improvement in five-phase unequal tooth SPM machine by injecting third harmonic current," *IEEE Trans. Veh. Technol.*, vol. 67, no. 1, pp. 206–215, Jan. 2018.
[16] B. Xu, Q. Jiang, W. Ji, and S. Ding, "An improved three-vector-based model predictive current control method for surface-mounted PMSM drives," *IEEE Trans. Transport. Electrific.*, vol. 8, no. 4, pp. 4418–4430, Dec. 2022.
[17] Q. Hou, S. Ding, X. Yu, and K. Mei, "A super-twisting-like fractional controller for SPMSM drive system," *IEEE Trans. Ind. Electron.*, vol. 69, no. 9, pp. 9376–9384, Sep. 2022.
[18] P. Zhao and G. Yang, "Torque density improvement of five-phase PMSM drive for electric vehicles applications," *J. Power Electron.*, vol. 11, no. 4, pp. 401–407, Jul. 2011.
[19] M. Fei and R. Zanasi, "Control of a five-phase synchronous motors with third harmonic constrained injection," in *Proc. 9th IEEE Int. Conf. Control Autom. (ICCA)*, Dec. 2011, pp. 957–962.
[20] Y. Sui, P. Zheng, Y. Fan, and J. Zhao, "Research on the vector control strategy of five-phase permanent-magnet synchronous machine based on third-harmonic current injection," in *Proc. IEEE Int. Electr. Mach. Drives Conf. (IEMDC)*, May 2017, pp. 1–8.
[21] G. Liu, C. Geng, and Q. Chen, "Sensorless control for five-phase IPMSM drives by injecting HF square-wave voltage signal into third harmonic space," *IEEE Access*, vol. 8, pp. 69712–69721, 2020.

JIANHUA LI was born in Heilongjiang, China, in 1994. He received the B.S. degree in electrical engineering from the Harbin Institute of Technology, Harbin, China, in 2016, where he is currently pursuing the Ph.D. degree in electrical engineering.

His research interests include multiphase motor drives, fault tolerance operation, and power electronics.

BOCHAO DU was born in Heilongjiang, China, in 1986. He received the B.S., M.S., and Ph.D. degrees in fault diagnosis of permanent-magnet synchronous motors from the Harbin Institute of Technology, Harbin, China, in 2009, 2011, and 2016, respectively.

He is currently with the Department of Electrical Engineering, Harbin Institute of Technology. His research interests include motor fault diagnosis and fault tolerance operation, motor parameter estimation, power electronics, and motor drivers.

TIANXU ZHAO was born in Heilongjiang, China, in 1987. He received the B.S., M.S., and Ph.D. degrees in multiphase motor design and optimization from the Harbin Institute of Technology, Harbin, China, in 2009, 2011, and 2021, respectively.

He is currently with the Department of Electrical Engineering, Harbin Institute of Technology. His research interests include the electromagnetic design of electric drive systems, thermal analysis, reliability analysis, and accelerated life tests.

YUAN CHENG received the B.S., M.Sc., and Ph.D. degrees in electrical engineering from the Harbin Institute of Technology, Harbin, China, in 2002, 2004, and 2009, respectively.

From 2009 to 2011, he carried out research on permanent-magnet electric variable transmission and its applications in HEVs in the frame of the Energy Modeling and Energy Management of Hybrid and Electric Vehicles (MEGEVH) Network, France. From 2012 to 2019, he was with PSA Peugeot Citroën, Paris, France, where he is responsible for the research on novel energetic conversion systems for automotive applications and the development of powertrain simulation tools. He is currently with the Department of Electrical Engineering, Harbin Institute of Technology. His research interests include the design and control of electric machines and the modeling and control of electric vehicles (EVs) and hybrid EVs (HEVs).

SHUMEI CUI was born in Heilongjiang, China, in November 1964. She received the Ph.D. degree in electrical engineering from the Harbin Institute of Technology (HIT), Harbin, China, in 1998.

She was a Professor with the Department of Electrical Engineering, HIT. Her research interests include the design and control of micro and special electric machines, the electric drive system of electric vehicles, the control and simulation of hybrid electric vehicles, and intelligent test and fault diagnostics of electric machines.

Dr. Cui is a member of the Electric Vehicle Committee and the National Automotive Standardization Technical Committee. She serves as the Vice Director Member for the Micro and Special Electric Machine Committee and the Chinese Institute of Electronics.